A nanotube based electron microbeam cellular irradiator for radiobiology research

David E. Bordelon,[1] Jian Zhang,[2] Sarah Graboski,[2] Adrienne Cox,[2] Eric Schreiber,[2] Otto Z. Zhou,[3] and Sha Chang[2,a)]

[1]*Curriculum in Applied and Materials Sciences, University of North Carolina, Chapel Hill, North Carolina 27599, USA*

[2]*Department of Radiation Oncology, University of North Carolina, Chapel Hill, North Carolina 27599, USA*

[3]*Department of Physics and Astronomy, Curriculum in Applied and Materials Sciences, and Lineberger Comprehensive Cancer Center, University of North Carolina, Chapel Hill, North Carolina 27599, USA*

(Received 13 August 2008; accepted 16 November 2008; published online 10 December 2008)

A prototype cellular irradiator utilizing a carbon nanotube (CNT) based field emission electron source has been developed for microscopic image-guided cellular region irradiation. The CNT cellular irradiation system has shown great potential to be a high temporal and spatial resolution research tool to enable researchers to gain a better understanding of the intricate cellular and intercellular microprocesses occurring following radiation deposition, which is essential to improving radiotherapy cancer treatment outcomes. In this paper, initial results of the system development are reported. The relationship between field emission current, the dose rate, and the dose distribution has been investigated. A beam size of 23 μm has been achieved with variable dose rates of 1–100 Gy/s, and the system dosimetry has been measured using a radiochromic film. Cell irradiation has been demonstrated by the visualization of H2AX phosphorylation at DNA double-strand break sites following irradiation in a rat fibroblast cell monolayer. The prototype single beam cellular irradiator is a preliminary step to a multipixel cell irradiator that is under development. © *2008 American Institute of Physics.* [DOI: 10.1063/1.3043417]

I. INTRODUCTION

The use of microbeam techniques in radiobiology has been an area of growing interest in recent years.[1,2] The prospect of studying the responses of cells to targeted radiation in real time provides great potential for understanding the elusive microprocesses taking place at the cellular level. Several microbeam irradiation methods have been developed, including charged particle irradiation,[3–5] x-ray irradiation,[6] as well as electron irradiation.[7–9] A charged particle microbeam system utilizes a particle accelerator to create a collimated beam of ions such as alpha particles, while an x-ray tube is commonly used to produce an x-ray microbeam through collimation. Electron microbeams have been produced based on commercially available thermionic electron guns. Size, cost, and use issues related to large centralized particle accelerator facilities make microbeam irradiators not easily accessible to many scientists in research laboratories. All the microbeam systems reported to date consist of only a single beam, requiring a fast alignment technique to irradiate large numbers of cells quickly.

We have undertaken an initiative to develop a pixelated or a multipixel electron microbeam irradiator for radiobiology research based on the recent advances in carbon nanotube (CNT) field emission technology.[10–12] CNTs have been widely studied as field emission electron sources for a variety of electronic devices including displays,[13,14] x-ray tubes,[15–17] and point electron source.[18] CNT based field emission cathodes have certain advantages over conventional thermionic cathodes in terms of low operating temperature, instantaneous response time, cathode design flexibility, and potential for miniaturization. Thus CNT field emission technology is ideal for the proposed multipixel electron microbeam cellular irradiation system, which is capable of high temporal and spatial resolution irradiation to user specified multiple cellular regions under microscope observation. Here we report the progress in the first phase of this development effort, which is design and construction of a single-pixel cellular irradiation system for feasibility demonstration. The detailed design and characterization of the system are described.

II. DESIGN AND EXPERIMENTAL METHODS

The CNT based single-pixel electron microbeam cellular irradiator, as illustrated in Fig. 1(a), contains a CNT field emission cathode, a metal mesh gate electrode, an electrostatic focusing lens, and an anode with a collimator and a semi-electron-transparent exit window. The CNT cathode used is a composite film deposited on a metal substrate by electrophoretic deposition (EPD) following the procedure we have published previously.[19,20] Small-diameter multiwall CNTs provided by Xintek were used as the starting material for the EPD ink. The CNT cathode used in this single beam system is a 1 mm diameter area of CNTs deposited onto a stainless steel substrate. The entire electron source is housed in a vacuum chamber maintained at 10^{-7} torr base pressure.

a)Author to whom correspondence should be addressed. Electronic mail: sha_chang@med.unc.edu.

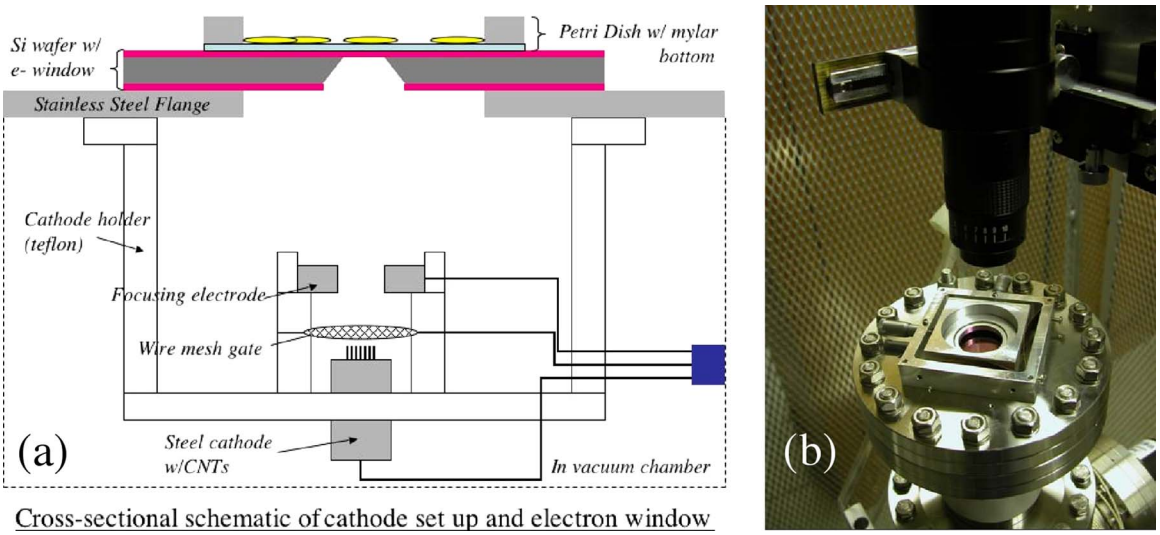

FIG. 1. (Color online) The single-pixel cellular irradiator system. (a) The cathode setup consists of a CNT field emission cathode serving as the electron source, a wire mesh gate to extract electrons from the CNTs, and a focusing electrode to electrically collimate the beam and shield the cathode from the high anode voltage. The electron window is formed from a silicon wafer with a chemical vapor deposited silicon nitride layer on the outside. A Mylar Petri dish sits atop the nitride window with its position movable via a simple translation stage. (b) An *x-y* translation stage was included to move the cell dish in relationship to the microbeam. A long working distance microscope positioned over the cell dish is used for cell alignment.

In this system the anode and cell stage are grounded and the cathode, chamber, pumps, and electronics are all floated at high negative voltage. The electron beam is extracted from the CNTs by applying a bias voltage on the gate electrode.[21] Collimation of the beam is achieved by applying a voltage to a focusing electrode above the gate as well as by physical collimation by the electron window. The electron beam penetrates through the electron window and irradiates the selected cell(s) on the cell dish. We have previously demonstrated similar CNT cathodes with excellent lifetime characteristics operating at high current for long durations.[22] Given the low currents (approximately 2 μA) and short pulse durations (typically with duty cycles 10% or less) needed in this cell irradiation system, the lifetime and stability of the CNT emitters are shown to be more than adequate. A single cathode has been used with negligible current drift in all of the testing and experiments performed with the system described here, spanning more than a year.

As shown in Fig. 1(b), a cell dish constructed of stainless steel and Mylar film was used to contain cells that are plated in a monolayer for irradiation. A 1.5 μm thick sheet of Mylar was glued to a flat bottomed stainless steel ring using a biologically compatible epoxy (EP21LV from Master Bond Inc.). It was placed on top of the silicon chip containing the silicon nitride exit window. An *x-y* translation stage was included to move the cell dish in relationship to the microbeam.

Alignment of the cells to the microbeam was achieved with the aid of a long working distance microscope positioned over the cell dish, as shown in Fig. 1(b). It was mounted over the system on a plexiglass frame to provide electrical insulation. The microscope was positioned over the grounded anode flange and the power and video feed from the charge-coupled device were connected to earth ground as well. The microscope mount included an *X-Y-Z* translation stage so that the microscope could be positioned relative to the window. Also a glass cover slip with an etched numbered grating was attached over the cell dish, but not in contact with the cells. As the cell dish was moved the microscope is fixed over the window and by changing the focus the position could be read from the etched cover slip.

Two types of electron transparent windows were fabricated to collimate and define the beam size. The first was made from a 400 μm thick silicon wafer with a deposited 300 nm silicon nitride (Si_3N_4) layer, following the steps illustrated in Fig. 2(a). Using photolithography, reactive ion etching (RIE), and potassium hydroxide anisotropic etching the wafer was etched from one side through to the other with the etch terminating on the silicon nitride. The KOH solution selectively etches certain crystal planes in the silicon leaving behind a 300 nm membrane at the bottom of an inverted pyramidal opening. The silicon contacts the silicon nitride with an angle of 54.7°. By defining the size of the etch pattern on the first side of the wafer the window size can be approximately determined. Using our current techniques square windows with side measurements of 20 ± 2 μm and smaller have been achieved, as illustrated in Fig. 2(b). These allow us to irradiate over relatively small areas. Additionally a 5 μm diameter laser drilled aperture in a 50 μm stainless steel foil was obtained. An ~2 μm Mylar film was affixed to the foil with adhesive to form a second type of window. The silicon nitride window chip and the laser drilled aperture/Mylar window were each attached to a central inset flange of the anode/irradiation stage.

During the irradiation, the field emission cathode was operated in the pulse mode. The pulse width, frequency, and count can be varied via the pulse generator, with pulse widths of 10 μs to 1 ms at 100 Hz being typical. The beam energy was fixed at 30 kV. Approximately 30% of the beam current was lost to the gate and focusing elements prior to reaching the anode surface, the electron window chip.[17,22] The transmission rate through the nitride membrane itself

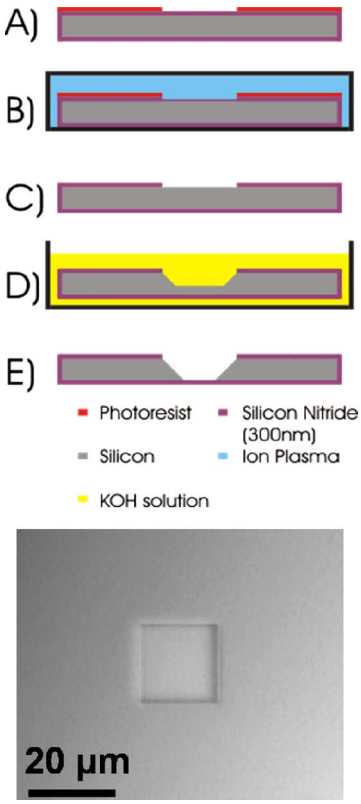

FIG. 2. (Color online) The fabrication process for the Si_3N_4 window is shown in this cross sectional rendering of the silicon wafer. (a) Patterning the photoresist with photolithography on the Si_3N_4 layer. (b) Etching the silicon nitride layer via RIE. (c) Substrate after RIE and photoresist removal, prior to KOH etching. (d) Etching the silicon substrate using KOH. (e) Completed KOH etching, showing the remaining silicon nitride membrane. The lower image is an optical microscope image of the silicon nitride window measuring ~18 μm on a side.

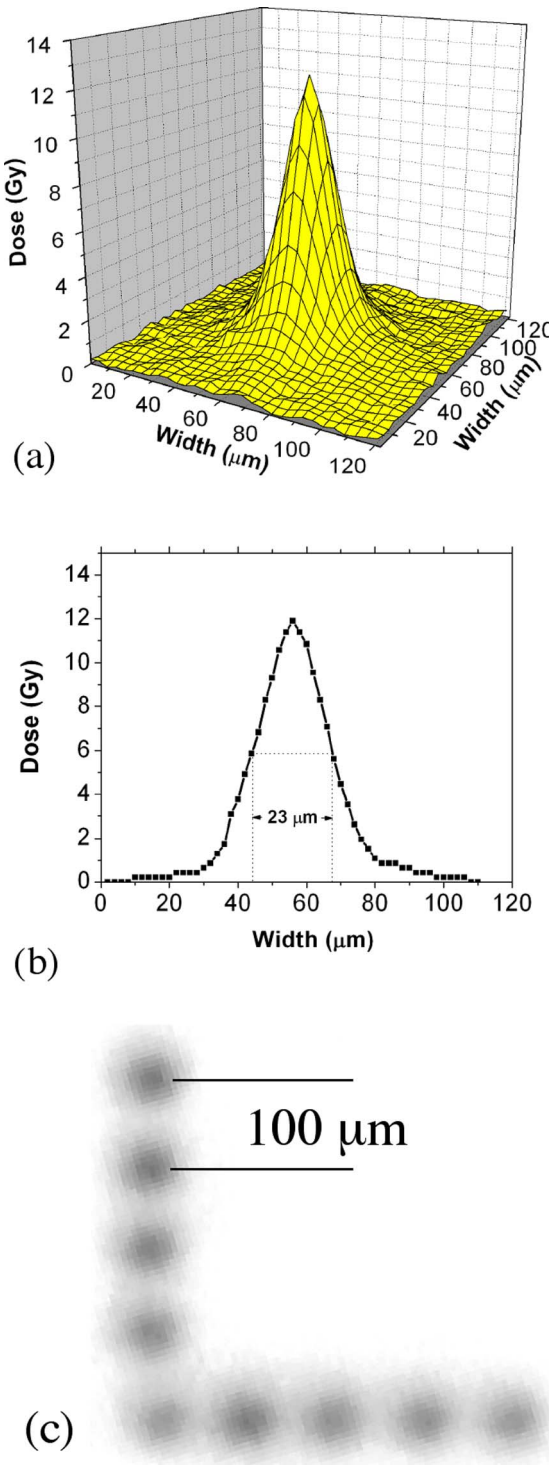

FIG. 3. (Color online) (a) 3D plot of dose as measured from scan of an electron irradiated radiochromic film. (b) Data cross section of a 3D plot. The peak exposure is 12 Gy with a FWHM of 23 μm. (c) Successive exposures in the radiochromic film were made following 100 μm movement via the simple translation stage to form the L shape seen above.

was determined to be at least 70% for a 30 keV electron beam.[23,24] The Mylar Petri dish bottom, which the electron beam must pass through before cell irradiation, also moderately attenuates the electron beam intensity.[25] However, the overall transmission rate of the system is largely determined by the size of the electron beam window/collimator chosen for a specific cell irradiation experiment. Conventional clinical radiotherapy and thus cell irradiation research use an average dose rate ranging from 1 to 300 Gy/h. With a 5 μm scale window we have produced a dose rate ranging from 1 to 100 Gy/s in the prototype system demonstrating that the field emission achieved is more than adequate for this application. Furthermore the measured current can be correlated with the dose delivered for any given cathode and electron window/collimator setup.

III. RESULTS

To calibrate the system a radiochromic film (GAF chromic HD-810) was used to determine the dose reaching the irradiation stage through the electron window. In this case the electron window used was the 5 μm diameter laser drilled aperture with the Mylar film electron window. The radiochromic film was then placed over the window and exposed in multiple locations. The film was subsequently scanned with the dosage determined from the optical density as compared to the background optical density. In this case a representative three-dimensional (3D) sample exposure plot is depicted in Fig. 3(a) showing the dose distribution determined from the scan of the film. The peak exposure is 12 Gy with a full width at half maximum (FWHM) of 23 μm, as illustrated in Fig. 3(b). Given the 5 μm diameter window size the FWHM measurement of 23 μm was somewhat

higher than expected. The beam size can be attributed to electron beam divergence and scattering in several locations. The moderate 10:1 aspect ratio of the laser drilled collimator, scattering in the Mylar layer, and the potential for thin air gaps between the layers of Mylar and radiochromic film all contribute to the beam size observed.

Next, a piece of a radiochromic film (Gafchromic HD-810) was rigidly attached to the bottom of the cell dish to simulate the process of irradiating various regions of a cell dish and to perform multiple irradiations in close proximity to one another. In this experiment an 18×18 μm silicon nitride electron window was used. The cell dish was then placed in the translation stage and the micrometers were manipulated so that the film could be irradiated in an "L-shaped" pattern as seen in Fig. 3(c). The film was shifted by 100 μm over the window between each irradiation exposure. Each exposure was a single millisecond pulse delivered with a cathode current of 2 μA and a beam energy of 30 kV. In this case an average maximum dose of 8.3 ± 0.9 Gy was achieved, demonstrating relative uniformity from exposure to exposure. Sources of variance could include lack of resolution in the film scanning process as well as varying nonzero gap distances between the electron exit window and the target, in this case the film. Also beam divergence through the silicon nitride window is broader because of the nonvertical sidewalls of the silicon collimator. While some beam broadening will occur via scattering, methods of reducing the beam size, such as reducing the window size and stacking two window chips together for increased collimation, are currently being pursued.

The system's cellular irradiation capabilities were demonstrated using rat fibroblast cells plated in sterile Mylar bottom cell dishes and the 18×18 μm silicon nitride window. The cells were maintained at standard incubation temperatures before and after the cell irradiation, which took about 20 min. A representative area of the SCI irradiated cell dish is depicted in Figs. 4(a) and 4(b) at 4× and 20×, showing the density of the plated cells. The cell dish was placed in the translation stage and positioned over the electron exit window. Using the micrometers the dishes were shifted 250 μm between irradiation doses in order to form an easily recognizable "L" shape. The irradiation location was noted via the etched glass cover slip for later examination. Following irradiation the cells were fixed and stained to visualize electron bombardment-induced DNA double-strand breaks (DSBs). A polyclonal antibody was used to detect foci of the phosphorylated histone gamma H2AX, which attaches to regions of DSBs. The cells were then examined with fluorescence microscopy as shown in Fig. 4(c). The areas fluorescing in green indicate the presence of foci of DSBs in the same location and in the same L-shaped pattern as expected. A positive control cell dish, uniformly irradiated in a cesium irradiator, is depicted in Fig. 4(d) showing uniform presence of foci across the dish. The combined data show that the amount of current generated by the CNT field emission is sufficient to quickly irradiate the cells to produce a clearly measurable response.

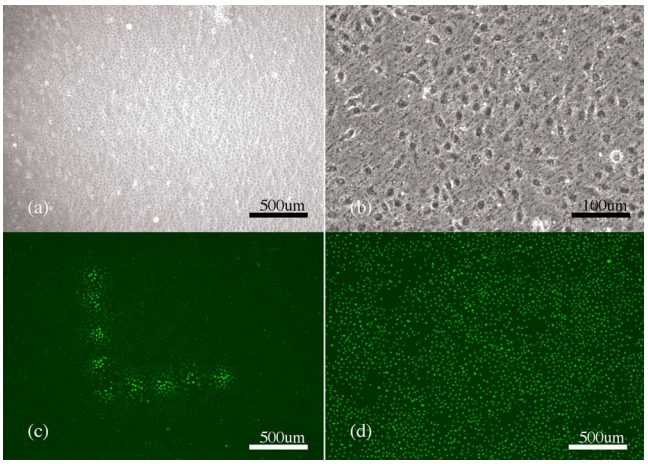

FIG. 4. (Color online) (a) and (b) Images of plated cells in Mylar bottom Petri dish at 4× and 20×, respectively, showing the cell density of the irradiation samples. (c) Fluorescent image of a plated cell sample following irradiation and fixing and staining procedure to mark DNA DSBs via the γ-H2AX, polyclonal fluorescent antibody. The separation between irradiation sites is approximately 250 μm. (d) Fluorescent image of a representative region of a positive control cell dish, uniformly irradiated in a cesium irradiator at 21 Gy, showing uniform presence of foci.

IV. SUMMARY

A novel microbeam cellular irradiator based on CNT field emission technology has been developed. This is the first reported instance of a cell irradiator utilizing nanotube technology, and while some issues remain to be resolved, we have demonstrated the feasibility of the system for unique cellular irradiation. The prototype system can deliver a dose range over several orders of magnitude with simple parameter changes. Furthermore, this system, by using micron dimension electron windows, has demonstrated the capability of irradiating cells over a specific area, which is also requisite to cell irradiation studies. The CNT based microbeam, utilizing nanotechnology and microfabrication methods, has potential for greater system miniaturization, opening the door to the production of more compact systems for additional end users without the large overhead usually associated with microbeam systems. The CNT based microbeam array, a multibeam system, currently under development will make possible the simultaneous irradiation of multiple sites by separate beams with temporal and dosage variance available for each beam. The advancement we report here along with the future possibilities mentioned each show promise for creating additional latitude, flexibility, and availability in microbeam irradiation.

ACKNOWLEDGMENTS

This work was supported by NIH (1R21CA118351-01) and the NC Biotechnology Center (2005MRG1111). We acknowledge helpful discussion with G. Johnson from Columbia University. D.E.B. and J.Z. made equal contribution to this work.

[1] S. Gerardi, Radiat. Prot. Dosim. **122**, 285 (2007).
[2] M. Sowa Resat and W. F. Morgan, Cancer Metastasis Rev. **23**, 323 (2004).

[3] M. Folkard, B. Vojnovic, K. M. Prise, A. G. Bowey, R. J. Locke, G. Schettino, and B. D. Michael, Int. J. Radiat. Biol. **72**, 375 (1997).
[4] P. Barberet, A. Balana, S. Incerti, C. Michelet-Habchi, P. Moretto, and T. Pouthier, Rev. Sci. Instrum. **76**, 015101 (2005).
[5] G. J. Ross, G. Garty, G. Randers-Pehrson, and D. J. Brenner, Nucl. Instrum. Methods Phys. Res. B **231**, 207 (2005).
[6] M. Folkard, G. Schettino, B. Vojnovic, S. Gilchrist, A. G. Michette, S. J. Pfauntsch, K. M. Prise, and B. D. Michael, Radiat. Res. **156**, 796 (2001).
[7] M. B. Sowa, M. K. Murphy, J. H. Miller, J. C. McDonald, D. J. Strom, and G. A. Kimmel, Radiat. Res. **164**, 695 (2005).
[8] J. H. Miller, M. T. Batdorf, D. J. Lynch, R. R. Lewis, and W. E. Wilson, Radiat. Res. **162**, 474 (2004).
[9] G. M. Sun, E. H. Kim, K. B. Song, and M. Jang, Radiat. Prot. Dosim. **121**, 84 (2006).
[10] S. Chang, J. Zhang, D. Bordelon, E. Schreiber, A. Cox, and O. Zhou, Radiat. Prot. Dosim. **122**, 323 (2007).
[11] S. Chang, J. Zhang, D. Bordelon, E. Schreiber, A. Cox, and O. Zhou, Radiat. Res. **166**, 658 (2006).
[12] S. Chang and O. Zhou, U.S. Patent No. 7,220,971 (May 22, 2007).
[13] W. B. Choi, D. S. Chung, J. H. Kang, H. Y. Kim, Y. W. Jin, I. T. Han, Y. H. Lee, J. E. Jung, N. S. Lee, G. S. Park, and J. M. Kim, Appl. Phys. Lett. **75**, 3129 (1999).
[14] S. Uemura, T. Nagasako, H. Kurachi, H. Yamada, T. Ezaki, T. Maesoba, T. Nakao, Y. Saito, and M. Yumura, J. Soc. Inf. Disp. **11**, 145 (2003).
[15] J. Zhang, Y. Cheng, Y. Z. Lee, B. Gao, Q. Qiu, W. L. Lin, D. Lalush, J. P. Lu, and O. Zhou, Rev. Sci. Instrum. **76**, 094301 (2005).
[16] J. Zhang, G. Yang, Y. Cheng, B. Gao, Q. Qiu, Y. Z. Lee, J. P. Lu, and O. Zhou, Appl. Phys. Lett. **84**, 1841041 (2005).
[17] G. Z. Yue, Q. Qiu, B. Gao, Y. Cheng, J. Zhang, H. Shimoda, S. Chang, J. P. Lu, and O. Zhou, Appl. Phys. Lett. **81**, 355 (2009).
[18] J. Zhang, J. Tang, G. Yang, Q. Qiu, L. C. Qin, and O. Zhou, Adv. Mater. (Weinheim, Ger.) **16**, 1219 (2004).
[19] B. Gao, G. Z. Yue, Q. Qiu, Y. Cheng, H. Shimoda, L. Fleming, and O. Zhou, Adv. Mater. (Weinheim, Ger.) **13**, 1770 (2001).
[20] S. J. Oh, J. Zhang, Y. Cheng, H. Shimoda, and O. Zhou, Appl. Phys. Lett. **84**, 3738 (2004).
[21] Z. Liu, J. Zhang, G. Yang, Y. Cheng, O. Zhou, and J. P. Lu, Rev. Sci. Instrum. **77**, 054302 (2006).
[22] Z. Liu, G. Yang, Y. Z. Lee, D. Bordelon, J. P. Lu, and O. Zhou, Appl. Phys. Lett. **89**, 103111 (2006).
[23] L. Hanlon, M. Greenstein, W. Grossman, and A. Neukermans, J. Vac. Sci. Technol. B **4**, 305 (1986).
[24] J. Wieser, D. E. Murnick, A. Ulrich, H. A. Huggins, A. Liddle, and W. L. Brown, Rev. Sci. Instrum. **68**, 1360 (1997).
[25] J. H. Miller, M. T. Batdorf, D. J. Lynch, R. R. Lewis, and W. E. Wilson, Radiat. Res. **162**, 474 (2004).